Geothermal Energy

RESEARCH Open Access

Performance of a hybrid heating system based on enhanced deep borehole heat exchanger and solar energy

Yujiang He[1,2] and Xianbiao Bu[3*]

*Correspondence:
buxb@ms.giec.ac.cn

[1] Institute of Hydrogeology and Environmental Geology, Chinese Academy of Geological Sciences, Shijiazhuang 050061, China
[2] Technology Innovation Center of Geothermal & Hot Dry Rock Exploration and Development, Ministry of Natural Resources, Shijiazhuang 050061, China
[3] Guangzhou Institute of Energy Conversion, Chinese Academy of Sciences, Guangzhou 510640, China

Abstract

Deep borehole heat exchanger (DBHE) is a closed loop system without the problem of fluid losses, scale formation and corrosion; however, low rock thermal conductivity limits its performance. Enlightened by drilling mud loss in oil and gas industry, here an enhanced DBHE (EDBHE) is proposed by filling materials with much higher thermal conductivity into leakage formation or depleted gas and oil reservoir to enhance the thermal conductivity performance of rock. Solar thermal energy is stored into EDBHE during the non-heating season to replenish the loss of heat energy extracted during the heating season. The results show that average heat mining rate for 20 years operations is, respectively, 3686.5 and 26,384.4 kW for EDBHE filled by ordinary drilling mud and by composite materials with high thermal conductivity. The percentage reduction of heat mining rate for 20 years operations for EDBHE and the hybrid system of geothermal and solar energy are, respectively, 16.1 and 5.8%, indicating that the hybrid system can make the heat mining rate more stable.

Keywords: Depleted oil and gas reservoir, Enhanced deep borehole heat exchanger, Leakage formation, Solar energy, Hybrid heating system

Introduction

Space heating in China requires tremendous amount of energy supply. At present, coal-based space heating is still the main force in north China, which contributes significantly to winter smog (Su et al. 2018). Geothermal energy already plays a vital role in space heating (Limberger et al. 2018; Moya et al. 2018), and it has provided heat for buildings with areas up to about 650 million m^2 by 2017 in China (Hou et al. 2018; Vanderzwaan and Longaa 2019). Recently, due to not relying on recharge technology and geothermal water resources, deep borehole heat exchanger (DBHE) is widely recognized (Nian and Cheng 2018), and many projects especially in China have been implemented (Bu et al. 2019a, b; Kohl et al. 2002; Morita et al. 1992).

For DBHE, many researches have been carried out from different perspectives including insulation tube, pump power, geothermal gradient, geological parameters, pipe diameter, injection parameters, thermal resistance, mathematical model, etc. With respect to insulation tube: Kujawa et al. (2006), Templeton et al. (2014), Śliwa et al. (2018) built

a numerical model about heat transfer to determine the performance of DBHE, and revealed the effects of vacuum-insulated tubing on heat production. With respect to pump power, Holmberg et al. (2016), Wight and Bennett (2015) studied the performance of DBHE and evaluated pump horsepower required to circulate the wellbore fluid. With respect to geothermal gradient, Pan et al. (2019), Caulk and Tomac (2017) discussed the effect of geothermal gradients on the thermal performance of DBHE. With respect to geological parameters, Cai et al. (2019), Morchio and Fossa (2019), Liu et al. (2020) investigated the influences of geological parameters on thermal extraction of DBHE. With respect to injection and extraction pipes, Noorollahi et al. (2015), Gharibi et al. (2018) researched the effects of pipe diameter, mass flow rate, fluid inlet temperature and insulation length on the extraction heat output. With respect to thermal resistance, Luo et al. (2019), Alimonti et al. (2019) studied the sensitivity towards borehole thermal resistance, fluid flow direction and geothermal gradient. With respect to rock temperature field, Morchio and Fossa (2020), Song et al. (2018) revealed the evolution of fluid and ground temperature as a function of some variable boundary conditions. With respect to injection parameters, Hu et al. (2020) and Nian et al. (2019) established a simulation model to evaluate and optimize the injection temperature. With respect to mathematical model, Luo et al. (2020), Fang et al. (2018) introduced and formulated a model for DBHE. DBHE is a closed loop system and working fluid has not direct contacts with surrounding rocks, which can avoid the fluid losses, scale formation and corrosion problem frequently presenting in the open-loop system.

The heat conduction from rock to well tube is the main heat transfer paths in the closed loop system of DBHE, which limits the improvement of system performance due to the poor thermal conductivity performance of rocks. The thermal conductivity coefficient of rocks generally ranges from 2.0 to 5.0 W/m/K according to different lithology, which is far smaller than that of well tube with the thermal conductivity coefficient of about 52 5.0 W/m/K. That is to say, the thermal resistance of rocks is far great than that of well tube, which causes heat energy to transfer from rocks to well tube more difficult. In fact, the heat transfer from rocks to well tube mainly includes three thermal resistances: rocks, cement and well tube thermal resistance, while the thermal resistance of rocks is the largest among the three. Thus, increasing thermal conductivity of rocks or reducing its thermal resistance is an effective method to enhance the system performance of DBHE. However, there is little research paper for the enhance of thermal conductivity of rocks. The aim of this study is to increase the thermal conductivity of rocks and reduce its thermal resistance.

In oil, gas and geothermal industry, drilling fluid or mud often flows into leakage formations (with high porosity and permeability) or fractures during drilling (Albattat and Hoteit 2019; Ezeakacha and Salehi 2018; Vipulanandan and Mohammed 2020). Drilling fluid loss concurrently happens during overbalanced drilling, and the drilling mud with fluid base tends to permeate into the porous formation around the well (Vipulanandan and Mohammed 2020). Okon et al. (2020) evaluated the use of locally sourced materials as fluid loss control additive in the water-based drilling fluid. Drilling fluid lost into formation damage and fractures induced by drill-in fluid loss is one of main problems of drilling well. Yan et al. studied the drill-in fluid loss mechanisms and the control of lost circulation in brittle gas shale located in the Longmaxi Formation, Sichuan Basin,

China (Yan et al. 2019). During the process of drilling, the temperature distributions of the formation and borehole under drilling fluid loss condition have a very important effect on the rheological design of drilling fluid, the borehole stability and the borehole pressure prediction. Zhang et al. (2020) calculated the distribution of borehole temperature when drilling fluid loss happens in the two-dimensional region at the bottom of hole during the process of drilling. Rock thermal conductivity can be improved if filler or drilling fluid with much higher thermal conductivity flows into depleted gas and oil reservoir or leakage formation. On this basis, a scheme on the enhanced deep borehole heat exchanger (EDBHE) is put forward in the current study, as shown in Fig. 1. When drilling geothermal well, drilling mud is generally adopted as the drilling fluid. In this study, composite filler with high thermal conductivity is used as the drilling fluid. Composite filler is firstly prepared through mixing carrier such as mud or cement slurry with some materials having high thermal conductivity such as graphene, carbon fiber or graphite. The density and viscosity of composite filler is adjusted by changing the content of each component in order to meet drilling fluid's functional needs. By adjusting back pressure, composite filler is controlled actively to fill into surrounding rocks when encountering leakage formation, fractures or depleted oil and gas reservoir. Filling composite materials such as graphene, carbon fiber or graphite with much higher thermal conductivity performance into depleted oil and gas reservoir, fractures or leakage formation can enhance the thermal conductivity of rocks as well as can create a low thermal resistance channel and thus can improve the heat extraction rate dramatically. With the increase of thermal conductivity of rocks in the fractures or leakage formation filled with composite materials having higher thermal conductivity, the heat extraction rate thus increases in these zones. However, the thermal conductivity of rocks without these zones is low, which cannot transfer heat energy rapidly into these zones due to poor thermal conductivity, thus leading to a rapid decrease of rock temperature in these zones due to the rapid heat energy extraction. Especially for long time operation, the heat extraction rate from the rocks will decrease if without heat energy compensation. Therefore, a new problem appears how to compensate thermal energy into EDBHE in order to ensure its stable and sustainable thermal output. Generally, there is enough place to install solar collectors in geothermal, oil or gas fields, and thus solar thermal energy is stored into EDBHE during the non-heating season to replenish the loss of heat energy extracted during the heating season. Therefore, a hybrid heating system of geothermal and solar energy is thus proposed in this study. The main purpose of this research is to calculate and evaluate the thermal performance of EDBHE and the hybrid heating system.

Mathematical model and experimental validation

System description

The shapes and sizes as well as spatial distribution of real leakage formation or depleted oil and gas reservoir is complicated, and it can be equivalent to the regular shape with uniform porosity for the convenience of calculation from the viewpoint of mathematics. Assuming that there are nine layers of the depleted oil and gas reservoir or leakage formation located from depth 2150 to 2555 m with uniform distribution (to simplify the schematic diagram, only two layers of leakage formation are given in Fig. 1), and the thickness for each layer is 5 m with average porosity of 0.2. For EDBHE, the horizontal well should be drilled in

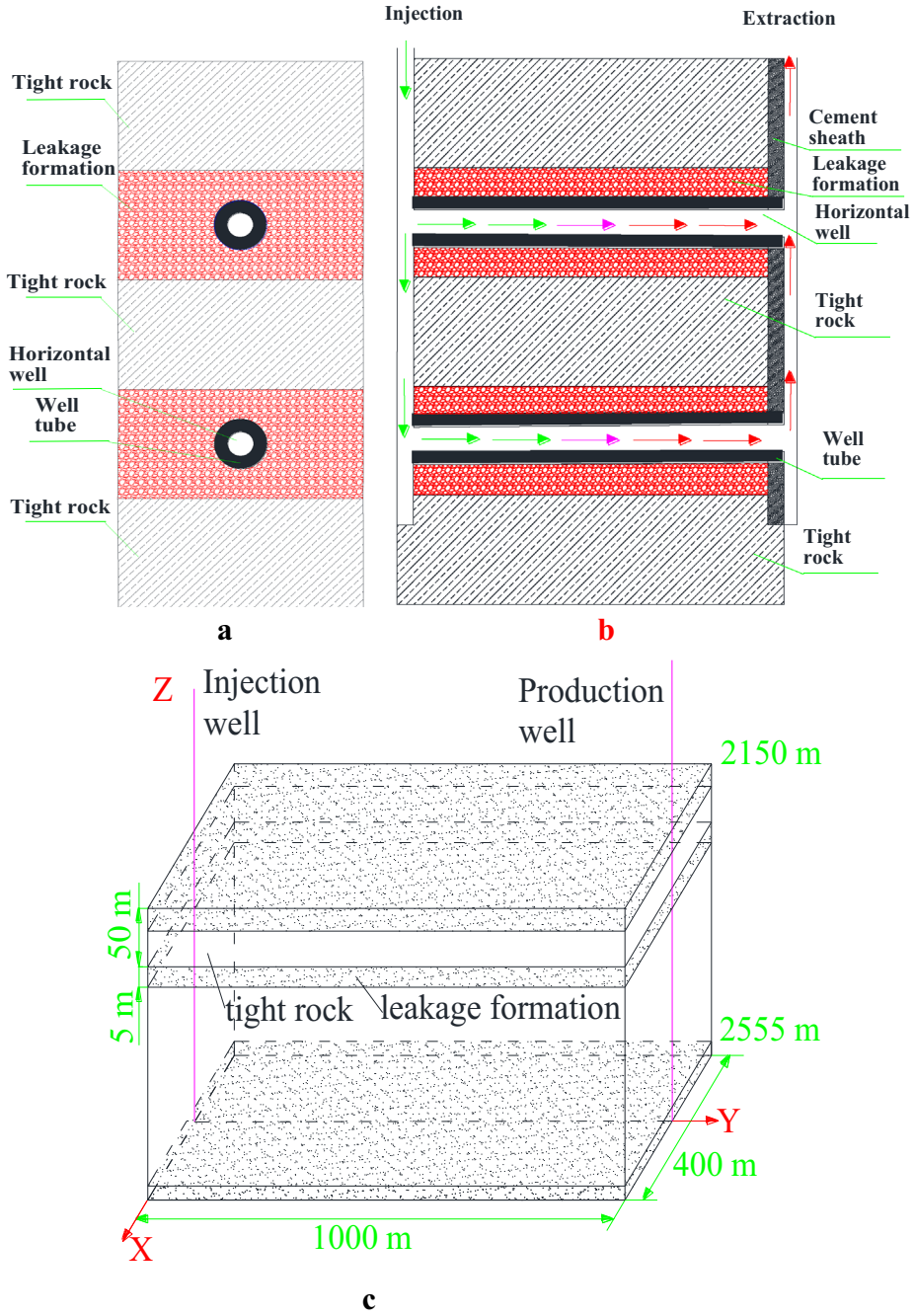

Fig. 1 Schematic of EDBHE. **a** Left view; **b** front view; **c** dimension

depleted oil and gas reservoir or leakage formation. The horizontal well has a length of 1000 m. The diameter for injection, extraction and horizontal wells is, respectively, 339.7, 339.7 and 177.8 mm, as shown in Fig. 1. The length, width and height of the packing space for composite filler in each layer of leakage formation are $1000 \times 400 \times 5$ m, as shown in Fig. 1c. The content of graphene added in composite filler are 50 wt%. Ordinary DBHE represents the deep borehole heat exchanger using ordinary drilling fluid without filling material with much higher thermal conductivity performance into leakage formation (ODBHE

for short). The parameters for ODBHE are the same as those of EDBHE except composite filler.

Assuming that well tube, cement and leakage formation or surrounding rocks has a good contact, thermal contact resistance is neglected between them. The mathematical model consists mainly of heat conduction equations in well tube, cement sheath, surrounding rocks or leakage formation and heat convection equation for working fluids inside the injection well and extraction well as well as horizontal wells.

Mathematical model

Heat conduction takes place in surrounding rocks, leakage formations, cement and well tube, while in injection, extraction and horizontal wells, heat convection is the main heat transfer patterns (Bu et al. 2019a, b; Caulk and Tomac 2017).

For injection well

$$\partial T_{\mathrm{i}}/\partial t + \partial(V_{\mathrm{i}}T_{\mathrm{i}})/\partial z = k_{\mathrm{l}}(T_{\mathrm{e}} - T_{\mathrm{i}})/(\rho A_{\mathrm{e}}c) + h_{\mathrm{w}}2\pi r_3(T_{\mathrm{wf}} - T_{\mathrm{i}})/(\rho A_{\mathrm{i}}c), \tag{1}$$

$$k_l = \frac{\pi}{\frac{1}{2h_{\mathrm{e}1}r_1} + \frac{1}{2\lambda_s}\ln\frac{r_2}{r_1} + \frac{1}{2h_{\mathrm{e}2}r_2}}, \tag{2}$$

where A_{i} represents flow area of injection well, m^2; c denotes specific heat of water, J/(kg·°C); the symbols $h_{\mathrm{e}1}$, $h_{\mathrm{e}2}$ and h_{w} are, respectively, convective heat transfer coefficient of insulation tube inner wall and outer wall as well as well tube inner wall, W/(m^2·°C); the symbols r_1 and r_2 represent, respectively, inner radius and outer radius of insulation pipe, m; λ_{s} denotes thermal conductivity of insulation pipe, W/(m·°C); r_3 denotes inner radius of well tube, m; T_{e} and T_{i}, respectively, represent fluid temperature in extraction well and injection well, °C; T_{wf} is well tube temperature, °C; k_{l} represents heat conductivity coefficient of unit length, W/(m·°C); V_{i} denotes flow velocity in injection well, m/s; ρ is water density, kg/m^3.

For extraction well

$$\partial T_{\mathrm{e}}/\partial t + \partial(V_{\mathrm{e}}T_{\mathrm{e}})/\partial z = -k_{\mathrm{l}}(T_{\mathrm{e}} - T_{\mathrm{i}})/(\rho A_{\mathrm{e}}c), \tag{3}$$

where V_{e} represents water velocity flowing in extraction well, m/s; A_{e} denotes flow area of extraction well, m^2.

In the horizontal well, the flow and heat transfer equation is the same as that in vertical well such as injection or extraction well.

Energy equation of cement

For cement, the energy equation is given as follows:

$$\frac{\partial T_{\mathrm{c}}}{\partial t} = \frac{\lambda_{\mathrm{c}}}{\rho_{\mathrm{c}}c_{\mathrm{c}}}\left(\frac{1}{r}\frac{\partial}{\partial r}\left(r\frac{\partial T_{\mathrm{c}}}{\partial r}\right)\right),\ r_4 \le r \le r_5, \tag{4}$$

where c_c represents cement's specific heat, J/(kg·°C); T_c denotes cement's temperature, °C; λ_c represents cement's thermal conductivity, W/(m·°C); ρ_c denotes the density of cement, kg/m^3; the symbols r_4 and r_5 represent cement's inner radius and outer radius, respectively, m.

Energy equation for surrounding rocks and leakage formations

$$\frac{\partial T_r}{\partial t} = \frac{\lambda_r}{\rho_r c_r}\left(\frac{1}{r}\frac{\partial}{\partial r}\left(r\frac{\partial T_r}{\partial r}\right) + \frac{\partial^2 T_r}{\partial y^2}\right),\ r_5 \le r \le r_\infty, \tag{5}$$

where T_r represents temperature of rocks or leakage formations, °C; λ_r denotes thermal conductivity coefficient, W/(m·°C); ρ_r denotes density, kg/m^3; c_r represents specific heat, J/(kg·°C).

Convective heat transfer coefficient (Zhang et al. 2001)

In injection well:

$$h = 0.023\lambda\ \mathrm{Re}^{0.8}\,\mathrm{Pr}^{0.4}\Big/ d_e. \tag{6}$$

In extraction well:

$$h_{e1} = 0.023\lambda\ \mathrm{Re}^{0.8}\,\mathrm{Pr}^{0.3}\Big/ (2r_1), \tag{7}$$

where d_e represents hydraulic diameter, m.

Initial and boundary conditions

The heat flux extracted by fluid through well wall is given as:

$$h_w(T_{wf} - T_i)\big|_{r=r_3} = \lambda_w \frac{\partial T_{wf}}{\partial r}\big|_{r=r_3}, \tag{8}$$

where λ_W denotes well wall's thermal conductivity, W/(m·°C).

Heat transfer from cement to well tube:

$$\lambda_w \frac{\partial T_{wf}}{\partial r}\big|_{r=r_4} = \lambda_c \frac{\partial T_c}{\partial r}\big|_{r=r_4}. \tag{9}$$

Heat transfer from leakage formations or rocks to cement:

$$\lambda_c \frac{\partial T_c}{\partial r}\big|_{r=r_5} = \lambda_r \frac{\partial T_r}{\partial r}\big|_{r=r_5}, \tag{10}$$

given that the rock temperature keeps undisturbed when $r > 200$ m (Song et al. 2018).

To enhance heat transfer, graphene filament (not powdered graphene) is used when preparing composite filler. The graphene content in composite filler is 50 wt%.

For composite filler, the thermal conductivity coefficient is given as follows:

$$\lambda_{\mathrm{cm}} = 0.5\lambda_{\mathrm{m}} + 0.5\lambda_{\mathrm{g}}, \tag{11}$$

where the symbols λ_{g}, λ_{m} and λ_{cm}, respectively, represent thermal conductivity of graphene, mud and composite filler, W/(m·K).

Assuming that the porosity in the leakage formation is 0.2, for leakage formation filled with composite materials, the thermal conductivity coefficient is given by:

$$\lambda_{\mathrm{cr}} = \frac{0.8\rho_{\mathrm{r}}\lambda_{\mathrm{r}} + 0.2\rho_{\mathrm{cm}}\lambda_{\mathrm{cm}}}{0.8\rho_{\mathrm{r}} + 0.2\rho_{\mathrm{cm}}}, \tag{12}$$

where ρ_{cm} is the density of composite filler.

The thermal resistance of rock or leakage formation is calculated according to the following formula:

$$R_{\mathrm{S}} = \frac{1}{2\pi\lambda_{cr}} \ln\frac{r_{\infty}}{r_5}, \tag{13}$$

where R_{S} is the thermal resistance, (m·K)/W; r_5 represents outer radius of cement, which is in direct contact with the rock or leakage formation.

The outer diameters for well tube and cement are, respectively, 339.7 mm and 444.5 mm.

R_{S} is, respectively, 141.8×10^{-3}, 49.5×10^{-3} and 4.9×10^{-3} (m·K)/W at $\lambda_{\mathrm{cr}} = 3.5$, 10 and 100 W/(m·K) from r_5 to $r_{\infty} = 5$ m.

R_{S} for cement is 58.6×10^{-3} (m·K)/W.

R_{S} for well tube is 2.8×10^{-4} (m·K)/W.

Two conclusions can be drawn through the above thermal resistance analysis (1) compared with well tube, rock and cement have big thermal resistance, which are two big obstacles to heat transfer from rock to well tube; (2) the thermal resistance of rock has the same order of magnitude as that of cement when the thermal conductivity of leakage formation filled with composite materials with higher conductivity increases from 3.5 to 10 W/(m·K). According to Eqs. (11) and (12), the thermal conductivity of high thermal conductivity materials such as graphene, carbon fiber or graphite shall not be lower than 75 W/(m·K) when the thermal conductivity of leakage formation equals to 10 W/(m·K).

The volume consumption of composite filler is calculated by

$$V_{\mathrm{cm}} = \pi R^2 \Delta H \varepsilon n, \tag{14}$$

where V_{cm} is the volume consumption of composite filler, m^3; R represents the extension distance of composite filling materials in the leakage formation in horizontal direction (in the radial direction), m; ΔH denotes the height of each layer leakage formation, $\Delta H = 5$ m; ε is the porosity of leakage formation, $\varepsilon = 0.2$; n is total layers of leakage formation, $n = 9$.

The parameters adopted in the simulation process are listed in Table 1. The heating duration for each year is 140 days in Qingdao, China, and the rest of time in the no-heating season is used to recover heat.

Table 1 Parameters used in simulation process

Parameter	Value
Surface temperature, °C	15.0
Geothermal gradient, °C/km	27.8
Vertical depth of well, m	2605
Rock's density of, kg/m^3	2800
Rock's specific heat, J/(kg·°C)	920
Rock's thermal conductivity, W/(m·°C)	3.5
Thermal conductivity of insulation pipe, W/(m·°C)	0.2
Density of mud, kg/m^3	1800
Insulation tube diameter, mm	110
Length of insulation tube, m	2600
Vertical well tube diameter, mm	339.7
Horizontal well tube diameter, mm	177.8
Thermal conductivity of graphene, W/(m·°C)	5300
Thermal conductivity of mud, W/(m·°C)	1.5
Cement's thermal conductivity, W/(m·°C)	0.7

Finite volume method is used to discretize Eqs. 1, 3, 4 and 5 with the implicit scheme (Li 2008), and then those equations are solved through TDMA (tri-diagonal matrix algorithm) algorithm (Tao 2001). The parameters used during the process of simulation are listed in Table 1.

Mathematical model for solar energy

The schematic of a hybrid heating system of geothermal combined with solar energy is shown in Fig. 2. In the hybrid heating system by combining geothermal with solar energy (hybrid system, for short), the evacuated tubular solar collector is selected, and the thermal efficiency for this type of collector can be calculated below (Li et al. 2016):

$$\eta = 0.721 - 0.89\frac{T_{\mathrm{m}} - T_0}{G} - 0.0199\frac{(T_{\mathrm{m}} - T_0)^2}{G}, \tag{15}$$

where η represents the thermal efficiency of evacuated tubular solar collector, T_{m} indicates average outlet and inlet temperature of solar collector °C; T_0 denotes ambient temperature, °C, G denotes the intensity of direct radiation, W/m^2. Solar direct radiation intensity reaches 750 W/m^2 for 7 h per day in the non-heating season with external average temperature of 21.2 °C, and it is 600 W/m^2 for 6 h per day in the heating season with external average temperature of 4.6 °C in Qingdao, China.

The total heat mining rate from hybrid system in the heating season is given as following:

$$P_{\mathrm{h}} = P_{\mathrm{g}} + P_{\mathrm{s}}, \tag{16}$$

where the symbols P_{s} and P_{g} denote the heat mining rate from solar collector and geothermal energy, respectively. P_{h} represents the total heat mining rate from hybrid system. In the heating season, the heat energy for buildings is provided by combining the geothermal system with solar energy system, and the intermittence of solar energy can be solved by adjusting the heat mining rate of geothermal energy. While the solar energy

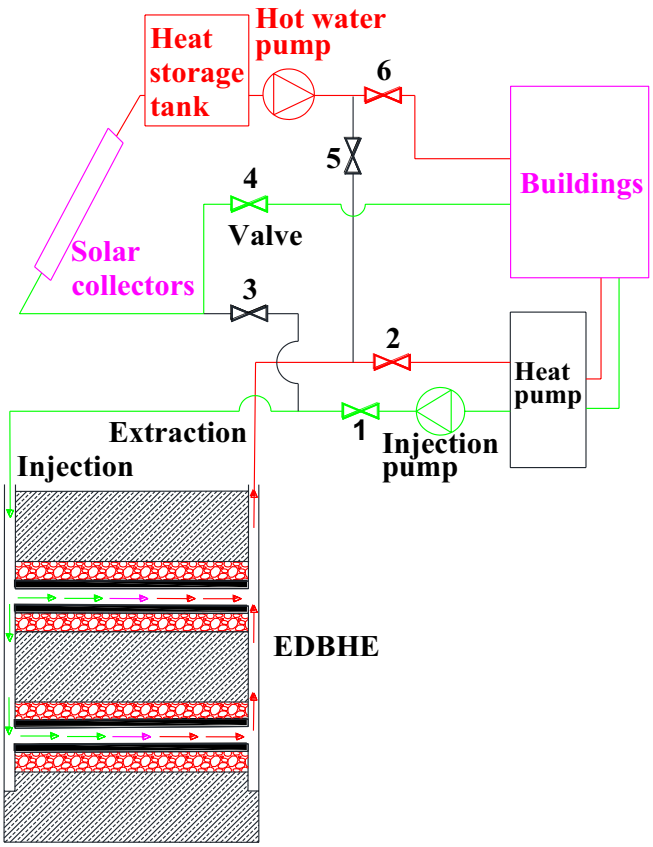

Fig. 2 A hybrid heating system of geothermal combined with solar energy

can store into geothermal reservoir in the non-heating season, compensating the loss of heat energy extracted in the heating season.

The storage tank just stores short-term heat energy on a diurnal basis in hybrid system. In heating season, the valves with sequence number of 1, 2, 4 and 6 are opened, and valves 3 and 5 kept closed. On the user sides, the supply and return water temperatures are 45 and 40 °C, respectively. For EDBHE, the injection water temperature is 5 °C in the heating season. Valves 3 and 5 are kept open, and valves with sequence number of 1, 2, 4 and 6 are shut off in non-heating season. The water temperature from solar collectors is 90 °C in the non-heating season.

Experimental validation

The experiment was conducted in Qingdao, China, from Nov. 19, 2017 to Apr. 6, 2018 in order to validate the mathematical model. The parameters used are listed in Table 1. The experiment subject is DBHE for only a vertical well without the horizontal well (Bu et al. 2019a, b). A comparison of numerical results with experimental data is described in Fig. 3. The temperature of injection water is at about 5 °C and the extraction water temperature is below 20 °C from Fig. 3. Therefore, heat pump units and DBHE are joined for supplying heat to buildings. In Fig. 3, the symbol T_{in} and T_{out}, respectively, represent temperature of injection and extraction water for DBHE or EDBHE. In the process of

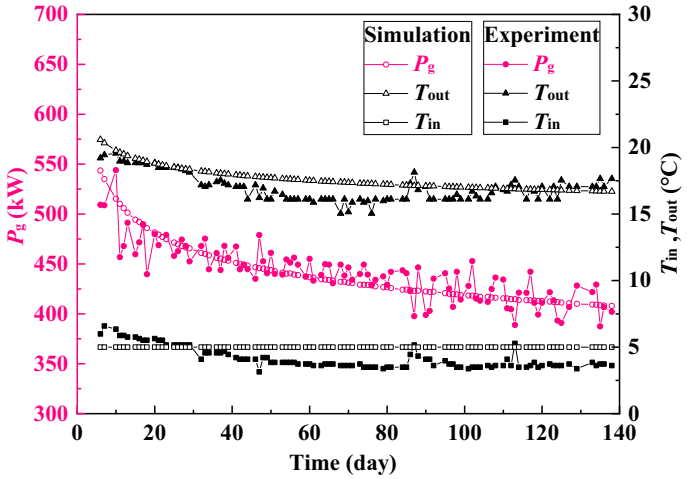

Fig. 3 Comparison of numerical results with experimental data

experiment, the flow rate of injection water is set at almost 30 m^3/h. It is obvious from Fig. 3 that the numerical results agree well with the experimental data. That is, the mathematical model validated through experiment on DBHE is reliable and can be adopted to calculate and evaluate the performance of EDBHE due to it having the same mathematical model as DBHE.

Results and discussion

The well depth for DBHE (please refer to the related references, Gharibi et al. 2018; Holmberg et al. 2016), and EDBHE is all 2600 m. The injection water temperature for DBHE and EDBHE is all 5 °C. For volume flow rate Q, it is 30 m^3/h for DBHE, while it is 342.1 m^3/h for EDBHE.

Figure 4a, b plots the variation of P_g and T_{out} with time for DBHE, ODBHE and EDBHE. From Fig. 4a, the average P_g for 20 years operations is, respectively, 417.7 and 26,384.4 kW for DBHE and EDBHE, demonstrating that filling high thermal conductivity composite materials into the depleted oil and gas reservoir or leakage formation improves the heat mining rate dramatically. The volume flow rate and injection water temperature for ODBHE are the same as those of EDBHE. The average heat mining rate for twenty years' operations is respectively, 3686.5 and 26,384.4 kW for ODBHE and EDBHE from Fig. 4b and Table 2, indicating that increasing thermal conductivity can indeed improve the heat mining rate. This is due to the fact that a channel with low thermal resistance is created through filling composite materials with much higher thermal conductivity into the depleted oil and gas reservoir or leakage formation, as a result, the heat stored in and around the depleted oil and gas reservoir or leakage formation preferentially transfers to the channel with a low thermal resistance and then to well wall through it. That is, the channel with a low thermal resistance is like a motorway built in the rugged region, through which the heat transfers much faster than that in DBHE. The fact of creating the channel with a low thermal resistance is also confirmed by rock temperatures, as shown in Fig. 5. Figure 5 shows that more heat energy stored in the rocks transfers into the well tube due to the enhancement of thermal conductivity, which can

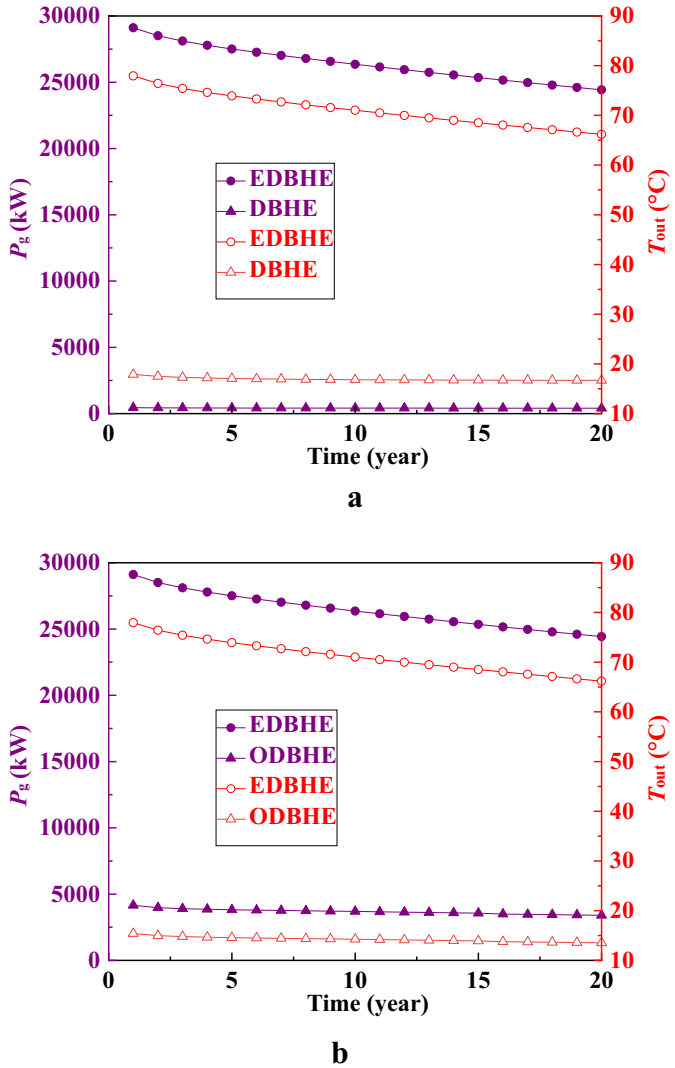

Fig. 4 Heat mining rate performance. **a** EDBHE and DBHE; **b** EDBHE and ODBHE

Table 2 Performance comparison of DBHE, ODBHE, and EDBHE

Name	Q, m^3/h	T_{in}, °C	Average Pg, kW
DBHE	30	5	417.7
ODBHE	342.1	5	3686.5
EDBHE	342.1	5	26,384.4

be reflected through the temperature drop of rocks in and around the leakage formation filled with composite material, as shown in Fig. 5c. In Fig. 5c, the heat energy stored in the rocks transfers into the well tube even though the rocks are far away from the well tube, while in Fig. 5b, c, only the heat energy of rocks near the well tube has the temperature drop due to the low thermal conductivity.

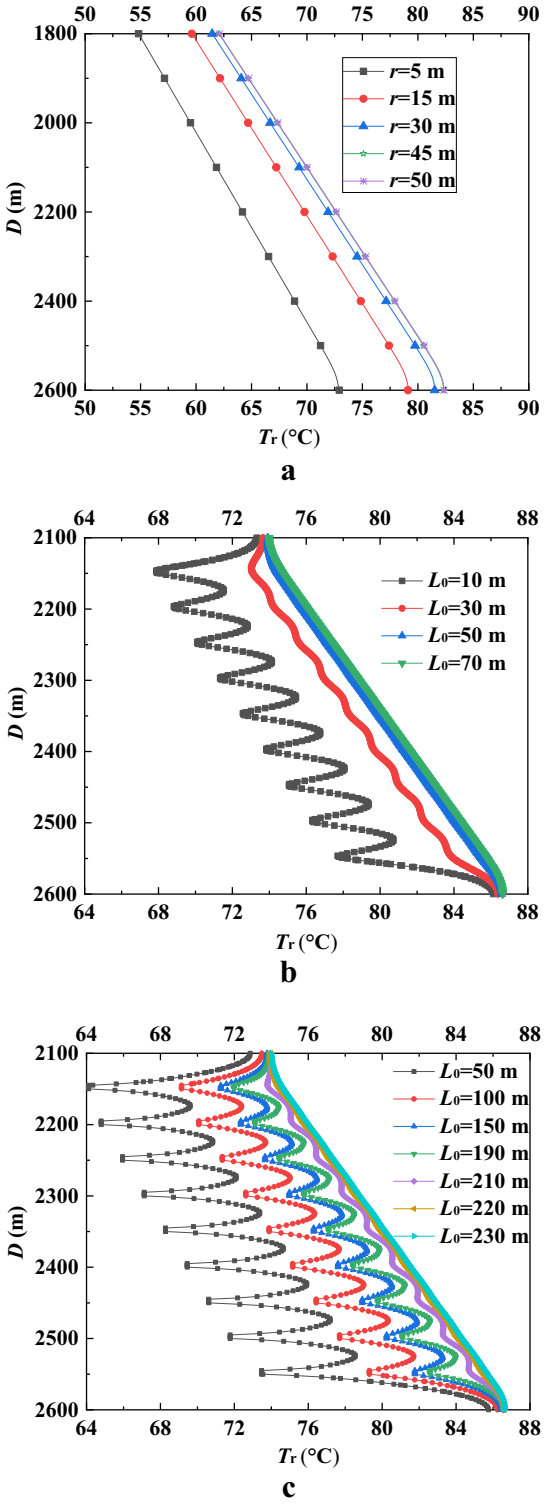

Fig. 5 Rock temperature. **a** DBHE; **b** ODBHE; **c** EDBHE

Figure 5 depicts the variation of rock temperatures as functions of depth and horizontal distance at the end of 20th heating season. D denotes well depth and L_0 is the distance of rock from the horizontal well in the horizontal direction (X direction, as shown in Fig. 1c). After 20 years of operation, the thermal influence distance for DBHE is only 45 m. It is obvious from Fig. 5b, c that the thermal influence distance for EDBHE and ODBHE reaches about 220 and 50 m, respectively, after 20 years of operation. As expected, the heat mining rate and extracted water temperature for EDBHE is greater than those for ODBHE and DBHE due to the existing of low thermal resistance channel.

From Fig. 4, the percentage reduction of P_g from 1st to 20th year is, respectively, 9.4% and 16.1% for DBHE and EDBHE. A solution to this problem of performance reduction is to use the hybrid system of geothermal and solar energy. Generally, there is enough place to install solar collectors in oil and gas or geothermal fields.

To determine the proper area of solar collectors, the load regulation capacity of geothermal energy should first be evaluated, as shown in Fig. 6. The volume flow rate and injection water temperature are kept invariable in all figures except Fig. 6. The effective adjustment measures mainly include the control of volume flow rate and injection water temperature. In Fig. 6, the symbols T_{in} and Q represent the temperature and volume flow rate of injection water, respectively. The load regulation capacity for EDBHE reaches up to 11,862.8 kW at $Q = 513.2$ m^3/h compared to that at $Q = 342.1$ m^3/h. From Fig. 6, it can be concluded that the volume flow rate has an important impact on P_g when comparing with T_{in}.

The hybrid heating system is shown in Fig. 2. In the hybrid system of EDBHE and solar energy, the evacuated tubular collector with area of 40,000 m^2 is planned to install according to the load regulation capacity. The symbol P_h in Fig. 7 denotes the total heat mining rate of the hybrid system.

In Fig. 7, the average P_g of 20 years are respectively 26384.4 and 28248.9 kW for EDBHE system and hybrid system. The percentage reduction of P_g from 1st to 20th year is, respectively, 16.1 and 5.8% in only EDBHE system and hybrid system, indicating that P_g in the hybrid system becomes more stable than that in only EDBHE system owing to

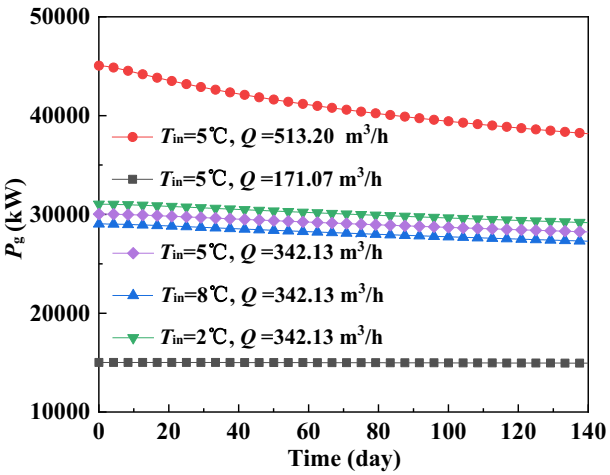

Fig. 6 Load regulation capacity of EDBHE

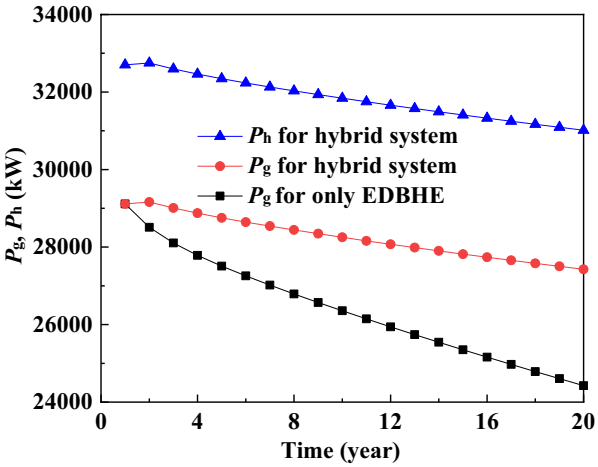

Fig. 7 Heat mining rate performance of EDBHE with solar energy

storing solar energy into geothermal reservoir. The average P_h for twenty years' operation is 31837.5 kW, which is 3588.6 kW greater than P_g in hybrid system. While the load regulation capacity of EDBHE reaches up to 11,862.8 kW at $Q = 513.2$ m^3/h compared to that at $Q = 342.1$ m^3/h, which is far greater than 3588.6 kW, indicating that more solar collectors can be installed in terms of the load regulation capacity of EDBHE. It can be concluded through analyzing Fig. 7 that solar energy can be stored into geothermal reservoir in non-heating season and the thermal energy can also be obtained from geothermal reservoir in the heating season due to filling composite materials with much higher thermal conductivity into depleted oil and gas reservoir (leakage formation). The above research results also show that four benefits can be achieved from the hybrid heating system ① the solar heat can be stored into geothermal reservoir without building seasonal thermal energy storage facility; ② the discontinuous and unstable energy supply problem for solar energy can be solved by adjusting the heat mining rate of geothermal energy; ③ the heat mining rate of geothermal energy in the hybrid system becomes more stable owing to storing solar energy into geothermal reservoir; and ④ the whole performance of the hybrid system is improved compared to the single geothermal heating system or the single solar energy heating system.

Conclusions

Deep borehole heat exchanger (DBHE) is one of the alternative technologies to acquire geothermal energy even though for dry hole; however, the low thermal conductivity of rocks is a major impediment to the enhancement of its performance. Fortunately, there are rich storage space and fracture pathway in some geothermal resources areas with leakage formations or in depleted oil and gas reservoir areas. Enlightened by drilling mud loss during the process of drilling in the gas and oil industry, a new scheme on enhanced deep borehole heat exchanger (EDBHE) is put forward by filling composite materials with high thermal conductivity into depleted oil and gas reservoir or leakage formations with the purpose of reducing rock's thermal resistance and enhancing the heat transfer performance. Graphene and carrier such as cement or clay or other

materials with low cost are used as raw materials to prepare composite filler. The price for graphene is high at this stage and however, it can also be replaced by other material with low price and high thermal conductivity such as carbon fiber.

For DBHE and EDBHE, the average P_g for 20 years of operations is, respectively, 417.7 and 26,384.4 kW, and the percentage reduction of P_g from 1st to 20th year is, respectively, 9.4% and 16.1%. For EDBHE combined with solar, the average P_g for twenty years' operation is 28248.9 kW, and the percentage reduction of P_g from 1st to 20th year is 5.8%, indicating that both heat mining rate and its performance reduction for hybrid system are better than those for single geothermal system.

Acknowledgements
This research is financially supported by the National Natural Science Foundation of China (No. 41972314) and by the "Transformational Technologies for Clean Energy and Demonstration", Strategic Priority Research Program of the Chinese Academy of Sciences, Grant No. XDA 21000000.

Author contributions
YH: conceptualization, formal analysis, methodology; XB: investigation, methodology, writing—original draft. Both authors read and approved the final manuscript.

Funding
The study was supported by National Natural Science Foundation of China (Grant No. 41972314).

Availability of data and materials
The datasets used and/or analyzed during this investigation are accessible upon reasonable request from the corresponding author.

Declarations

Competing interests
The authors declare that they have no competing interests.

Received: 4 June 2022 Accepted: 15 October 2022
Published online: 28 October 2022

References

Albattat R, Hoteit H. Modeling yield-power-law drilling fluid loss in fractured formation. J Petrol Sci Eng. 2019;182: 106273.
Alimonti C, Conti P, Soldo E. A comprehensive exergy evaluation of a deep borehole heat exchanger coupled with a ORC plant: the case study of Campi Flegrei. Energy. 2019;189: 116100.
Bu XB, Ran YM, Zhang DD. Experimental and simulation studies of geothermal single well for building heating. Renew Energy. 2019a;143:1902–9.
Bu XB, Jiang KQ, Li HS. Performance of geothermal single well for intermittent heating. Energy. 2019b;186: 115858.
Cai WL, Wang FH, Liu J, et al. Experimental and numerical investigation of heat transfer performance and sustainability of deep borehole heat exchangers coupled with ground source heat pump systems. Appl Therm Eng. 2019;149:975–86.
Caulk RA, Tomac I. Reuse of abandoned oil and gas wells for geothermal energy production. Renew Energy. 2017;112:388–97.
Ezeakacha CP, Salehi S. Experimental and statistical investigation of drilling fluids loss in porous media-part 1. J Nat Gas Sci Eng. 2018;51:104–15.
Fang L, Diao NR, Shao ZK, et al. A computationally efficient numerical model for heat transfer simulation of deep borehole heat exchangers. Energy Build. 2018;167:79–88.
Gharibi S, Mortezazadeh E, Bodi SJHA, et al. Feasibility study of geothermal heat extraction from abandoned oil wells using a U-tube heat exchanger. Energy. 2018;153:554–67.
Holmberg H, Acuna J, Næss E, et al. Thermal evaluation of coaxial deep borehole heat exchangers. Renew Energy. 2016;97:65–76.
Hou J, Cao M, Liu P. Development and utilization of geothermal energy in China: current practices and future strategies. Renew Energy. 2018;125:401–12.
Hu XC, Banks J, Wu LP, et al. Numerical modeling of a coaxial borehole heat exchanger to exploit geothermal energy from abandoned petroleum wells in Hinton, Alberta. Renew Energy. 2020;148:1110–23.
Kohl T, Brenni R, Eugster W. System performance of a deep borehole heat exchanger. Geothermics. 2002;31:687–708.
Kujawa T, Nowak W, Stachel AA. Utilization of existing deep geological wells for acquisitions of geothermal energy. Energy. 2006;31:650–64.
Li RX. Basis of finite volume method. 2nd ed. Beijing: National Defense Industry Press; 2008.
Li PC, Li J, Pei G, et al. A cascade organic Rankine cycle power generation system using hybrid solar energy and liquefied natural gas. Sol Energy. 2016;127:136–46.

Limberger J, Boxem T, Pluymackers M, et al. Geothermal energy in deep aquifers: a global assessment of the resource base for direct heat utilization. Renew Sust Energy Rev. 2018;87:44–60.
Liu J, Wang FH, Cai WL, et al. Numerical investigation on the effects of geological parameters and layered subsurface on the thermal performance of medium-deep borehole heat exchanger. Renew Energy. 2020;149:384–99.
Luo YQ, Guo HS, Meggers F, et al. Deep coaxial borehole heat exchanger: analytical modeling and thermal analysis. Energy. 2019;185:1298–313.
Luo YQ, Yu JH, Yan T, et al. Improved analytical modeling and system performance evaluation of deep coaxial borehole heat exchanger with segmented finite cylinder-source method. Energy Build. 2020;212: 109829.
Morchio S, Fossa M. Thermal modeling of deep borehole heat exchangers for geothermal applications in densely populated urban areas. Therm Sci Eng Progr. 2019;13: 100363.
Morchio S, Fossa M. On the ground thermal conductivity estimation with coaxial borehole heat exchangers according to different undisturbed ground temperature profiles. Appl Therm Eng. 2020;173: 115198.
Morita K, Bollmeier WS, Mizogami H. Experiment to prove the concept of the downhole coaxial heat exchanger (DCHE) in Hawaii. Geotherm Resour. 1992;16:9–16.
Moya D, Aldas C, Kaparaju P. Geothermal energy: power plant technology and direct heat applications. Renew Sust Energy Rev. 2018;94:889–901.
Nian YL, Cheng WL. Insights into geothermal utilization of abandoned oil and gas wells. Renew Sust Energy Rev. 2018;87:44–60.
Nian YL, Cheng WL, Yang XY, et al. Simulation of a novel deep ground source heat pump system using abandoned oil wells with coaxial BHE. Int J Heat Mass Transf. 2019;137:400–12.
Noorollahi Y, Pourarshad M, Jalilinasrabady S, et al. Numerical simulation of power production from abandoned oil wells in Ahwaz oil field in southern Iran. Geothermics. 2015;55:16–23.
Okon AN, Akpabio JU, Tugwell KW. Evaluating the locally sourced materials as fluid loss control additives in water-based drilling fluid. Heliyone. 2020;6:04091.
Pan AQ, Lu L, Cui P, et al. A new analytical heat transfer model for deep borehole heat exchangers with coaxial tubes. Int J Heat Mass Transf. 2019;141:1056–65.
Śliwa T, Kruszewski M, Zare A, et al. Potential application of vacuum insulated tubing for deep borehole heat exchangers. Geothermics. 2018;75:58–67.
Song XZ, Wang GS, Shi Y, et al. Numerical analysis of heat extraction performance of a deep coaxial borehole heat exchanger geothermal system. Energy. 2018;164:1298–310.
Su C, Madani H, Palm B. Heating solutions for residential buildings in China: current status and future outlook. Energy Convers Manag. 2018;177:493–510.
Tao WQ. Numerical heat transfer. 2nd ed. Xi'an: Xi'an Jiao tong University Press; 2001.
Templeton JD, Ghoreishi-Madiseh SA, Hassani F, Al-Khawaja MJ. Abandoned petroleum wells as sustainable sources of geothermal energy. Energy. 2014;70:366–73.
Vanderzwaan B, Longaa FD. Integrated assessment projections for global geothermal energy use. Geothermics. 2019;82:203–11.
Vipulanandan C, Mohammed A. Effect of drilling mud bentonite contents on the fluid loss and filter cake formation on a field clay soil formation compared to the API fluid loss method and characterized using Vipulanandan models. J Petrol Sci Eng. 2020;189: 107029.
Wight NM, Bennett NS. Geothermal energy from abandoned oil and gas wells using water in combination with a closed wellbore. Appl Therm Eng. 2015;89:908–15.
Yan XP, Kang YL, You LJ, et al. Drill-in fluid loss mechanisms in brittle gas shale: a case study in the Longmaxi Formation, Sichuan Basin, China. J Petrol Sci Eng. 2019;174:394–405.
Zhang XM, Ren ZP, Mei FM. Heat transfer. 4th ed. Beijing: China Construction Industry Press; 2001.
Zhang Z, Xiong YM, Pu H, et al. Borehole temperature distribution when drilling fluid loss occurs in the two-dimensional area at the bottom-hole during drilling. J Nat Gas Sci Eng. 2020;83:103523.

Publisher's Note